

Long-coding RNA ANRIL knockdown improves diabetes-induced renal injury

Xiaoming Jiang¹, Nan Su², Jiao Ding¹, Juean Jiang¹, Liqiang Yu¹, Yan Xie¹

¹General Medicine Department, The First Affiliated Hospital of Soochow University, Suzhou, China

²Department of Respiratory and Critical Care Medicine, The First Affiliated Hospital of Soochow University, Suzhou, China

Submitted: 12 January 2021

Accepted: 11 March 2021

Arch Med Sci

DOI: <https://doi.org/10.5114/aoms/134197>

Copyright © 2021 Termedia & Banach

Corresponding author:

Yan Xie

General Medicine

Department

The First Affiliated

Hospital of Soochow

University

Suzhou, China

E-mail: xieyan200120@163.com

com

Abstract

Introduction: The aim of the study was to investigate the effects and mechanisms of long non-coding RNA (lncRNA) in diabetes-induced renal injury, both *in vivo* and *in vitro*.

Material and methods: Sixty healthy subjects and 30 patients with diabetic nephropathy (DN) were enrolled in this study. The lncRNA ANRIL expression was measured by RT-qPCR assay in serum. Further, the ANRIL expression in kidney tissue of normal, 10-day DN, and 20-day DN rat models was measured. ELISA was used to measure levels of lactate dehydrogenase (LDH), malondialdehyde (MDA), superoxide dismutase (SOD), interleukin-6 (IL-6), and tumor necrosis factor (TNF)- α . Renal pathology was evaluated by hematoxylin-eosin (HE) staining, cell apoptosis by TUNEL assay, relative protein expression by immunohistochemical (IHC) assay, and relative mRNA expression by RT-qPCR assay. In the cell experiments, LDH, MDA, SOD, IL-6, and TNF- α levels were measured by enzyme-linked immunosorbent assay (ELISA); cell proliferation by Cell Counting Kit-8 (CCK-8); cell apoptosis by flow cytometry; and relative mRNA and protein expression by real-time quantitative polymerase chain reaction (RT-qPCR) and Western blot (WB) assay. The nuclear factor κ B (NF- κ B) (p65) nuclear volume of difference groups was evaluated by cell immunofluorescence.

Results: lncRNA ANRIL was significantly higher in DN patients than healthy subjects. Compared with the sham group, the ANRIL expression and LDH, MDA, IL-6 and TNF- α concentrations were significantly increased, and SOD concentrations and cell apoptosis rate were significantly decreased with increasing time. Toll-like receptor 4 (TLR4), myeloid differentiation factor 88 (MyD88), and NF- κ B(p65) mRNA and protein expression levels were significantly up-regulated.

Conclusions: lncRNA ANRIL knockdown could improve diabetes-induced renal injury via regulation of TLR4/NF- κ B(p65).

Key words: ANRIL, kidney injury, cell apoptosis, TLR4, MyD88, NF- κ B(p65).

Introduction

Long non-coding RNA (lncRNA) refers to RNA that has a length of > 200 nucleotides and cannot perform protein coding in the absence of a specific complete open reading frame [1]. Similar to mRNA, most lncRNAs not only possess a 5'-cap and 3'-tail structure but also undergo alternative splicing [2]. As a regulator for cell-specific gene expression,

lncRNA is widely involved in biological processes including gene expression and transcription, epigenetic regulation, cell cycle control, cellular differentiation, and immunoreactions.

As indicated by several research studies, lncRNA possesses more complex spatial structures and biological functions than miRNA. Thus, lncRNA regulation is more complicated, but also more accurate and more agile [3]. It was once deemed that ribonuclease in the plasma makes lncRNA present unstably. However, lncRNA has been recently demonstrated to be stably present in human blood plasma and other body fluids [4]. More significant expression and spatio-temporal specialization are found in lncRNA changes than with those of mRNA in disease progression [5]. Recent research has proven that lncRNA may act as a biomarker of disease diagnosis. According to the findings of Yang *et al.* [3] and Zhou *et al.* [6], plasma lncRNA AC100865.1 and lncRNA H19 can be selected as early diagnostic markers of coronary diseases and stomach cancer, respectively. In 2002, de Kok *et al.* [7] proved that prostate-specific lncRNA PCA3 (DD3) exists stably in urine. DD3 shows higher sensitivity and specificity than prostate-specific antigen (PSA) that is adopted for prostatic cancer diagnosis. Accordingly, PCA3 has been approved by the FDA as a diagnostically pertinent lncRNA.

Although several lncRNAs have been demonstrated to be involved in the progression of diabetic nephropathy (DN), no lncRNA has yet been clinically applied as a diagnostic and prognostic molecular marker. Based on differently expressed lncRNA in blood extracted from 60 patients with type 2 diabetes (T2D) and 60 healthy persons, Li *et al.* [8] reported that lncRNA ENST00000550337.1 was of extremely high significance for diagnosis of T2D and prediabetes. Tang *et al.* [5] performed sequencing analysis on epithelial cells in the proximal renal tubule of DN mice. According to their analytical results, spatio-temporal and expression specificity of lncRNA was more significant than that of mRNA in disease progression. Such a phenomenon indirectly signifies that lncRNA, as a molecular marker, outperforms mRNA.

In line with recent investigations, lncRNA ANRIL plays a vital role in inflammation and organ damage caused by inflammation [9–11]. Despite that, the mechanism of action of ANRIL in renal injuries caused by diabetes remains to be clarified. To our best knowledge, this is the first study to investigate and report the expression variations of lncRNA ANRIL in the plasma of healthy subjects and patients with DN. Subsequently, its mechanism of action was verified through *in vitro* experiments.

Material and methods

Clinical data

From January 2016 to December 2018, 30 patients with T2D complicated with DN (mean age: 56.5 ± 3.7 years) ($n = 15$ microalbuminuria and $n = 15$ high-grade proteinuria) were enrolled from our hospital. Depending on urinary albumin excretion rate (UAER) = 200 $\mu\text{g}/\text{min}$, the DN patients were divided into microalbuminuria and high-grade proteinuria. Additionally, 60 non-diabetic healthy people (mean age: 54.7 ± 6.4 years) who attended our physical examination center were selected as the control group. As approved by the Ethics Committee of the hospital, informed consent was obtained from all research subjects. In this case, 5 ml of venous blood was collected from all participants. After being stored for 30 min at 4°C , it was further subjected to centrifugation at $3000\times g$ for 15 min at ambient temperature. Afterwards, the serum was separated and stored at -80°C until further analysis. This study was approved by the Ethics committee of the First Affiliated Hospital of Soochow University (No. 2015120623), and patients gave written or verbal informed consent.

Animals

Thirty specific pathogen-free (SPF) male Wistar rats (body weight: 200–220 g) were purchased from Beijing Vitalriver Laboratory Animal Technology Co., Ltd. (certification No.: SCXK(Jing) 2018-0009).

Establishment of DN rat model

Twenty Wistar rats were fed with high-fat diet for 4 weeks. Then, streptozotocin (STZ) solution was intraperitoneally injected at a dose of 35 mg/kg after they were fasted for 12 h. Finally, the DN rat model was established. The rats in the sham group ($n = 10$) were treated with the same amount of normal saline instead of STZ solution. After 72 h, the blood glucose level of rats after 2-h glucose loading was measured. If the blood glucose level was > 11.1 mmol/l, the DN model was considered to have been successfully established.

Grouping and sampling

After successful DN modeling, the rats were further fed with high-fat diet for another 20 days. In this period, 10 rats were randomly selected and executed for the purpose of sampling on the 10th and 20th days. The remaining 10 Wistar rats were classified as the normal group and fed a normal diet. After 20 days, these 10 rats were also killed for further sampling and analysis.

The body masses of rats in different groups were measured at the designated time. After an-

esthesia with chloral hydrate, 4 ml of blood was drawn from the abdominal aorta. After centrifugation, serum was separated and stored at -20°C for lactate dehydrogenase (LDH), malondialdehyde (MDA), superoxide dismutase (SOD), interleukin-6 (IL-6), and tumor necrosis factor (TNF)- α testing. The rats were immobilized to open their chests and fully expose their hearts. Phosphate buffer was imported through incubation in their ventriculus sinister. After their kidneys turned white, they were taken out to be weighed for computing the kidney index. Some of the kidney tissue was fixed in 10% formalin solution to observe pathomorphism and for immunohistochemical staining. The left kidney tissues were stored in another refrigerator at -80°C for RT-PCR testing. Animals were treated in accordance with the Guide for the Care and Use of Laboratory Animals (8th edition, National Academies Press).

High-glucose cell model building and grouping

Briefly, 70–80% confluent cultured HK-2 cells (ATCC, USA) were digested and subcultured with trypsin containing EDTA. After cell ceiling trypsinization, the cells were synchronized for 24 h in a serum-free, low-sugar DMEM culture medium. With the addition of high glucose (final mass concentration: 30 mmol/l), they were cultured in 5% CO_2 at 37°C for 72 h.

The HK-2 cells were divided into the following groups: NC (normal control), Model, shNC, and shRNA. HK-2 in the NC group was cultured with a normal culture medium, while those in the Model, shNC, and shRNA groups were all cultured in high glucose culture media. Further, cell transfection in the shNC group underwent blank control, and shRNA was used to carry out shRNA-ANRIL transfection.

LDH, MDA, SOD, IL-6, and TNF- α determination

Cryopreserved serum or cell supernatant was thawed before ELISA. The concentrations of LDH, MDA, SOD, IL-6, and TNF- α were measured using respective ELISA kits (all Jiangsu KeyGENE Bio-TECH Co., Ltd; Nanjing, China), according to the manufacturer's instructions.

Pathomorphism of kidney tissues

Kidney tissues of rats in different groups were fixed for 24 h in 10% formalin and cut into 2- μm -thick tissue slices to be placed in a disposable wax box. After washing three times with distilled water, the tissue slices successively underwent ethyl alcohol gradient elution, dimethylbenzene transparentizing, and wax dip, after which paraffin embedding was performed. Hematoxylin-eosin (HE)

staining was also performed by a conventional method to observe changes in pathomorphism of kidney tissues.

TUNEL staining

Likewise, kidney tissues of rats in different groups were fixed for 24 h in 10% formalin and cut into 2- μm -thick tissue slices. The sections were deparaffinized in xylene. Subsequent to ethyl alcohol gradient elution, the sections were treated with protease K at $20\text{--}37^{\circ}\text{C}$ for 15–30 min. After PBS rinsing, HK-2 cell were incubated for 20 min at ambient temperature in 3% H_2O_2 and then rinsed in PBS. Next, biotin labeling, color development, and hematoxylin counterstaining were performed as per the kit specifications. The paraffin sections were washed in tap water and subjected to ethyl alcohol gradient elution and dimethylbenzene transparentizing, after which they were mounted in neutral resin. Finally, the sections were observed and photographed microscopically. Nuclei with brown granules were deemed as apoptotic cells.

Immunohistochemistry (IHC)

Deparaffinized and rehydrated paraffin sections were treated with 1% Triton X-100 for 15 min and then with 3% H_2O_2 for another 15 min. After blocking in 5% sheep serum for 30 min, the tissue sections were incubated in primary antibodies (4°C , overnight) and secondary antibodies (37°C , 30 min) for IHC staining. After the reaction was terminated, ImageJ software was used to analyze the protein expressions.

In-situ hybridization (ISH)

After dewaxing and hydration of the tissue sections, they were incubated for 15 min with protease (15 mg/l) at 37°C . Chips that had undergone ethyl alcohol gradient elution were placed in an environment of 55°C and subjected to pre-hybridization for 30 min; subsequently, a denatured digoxigenin-labelled cDNA probe lncRNA ANRIL (Exiqon in Denmark, 1 : 500) at 90°C was added into the hybridization working solution for overnight incubation at 55°C . Subsequent to gradient development and mounting the next day, anti-DIG-AP (1 : 800) was added for an hour-long incubation at an ambient temperature. Finally, NBT/BCIP was selected to perform staining. Mounting and microscopic examination were conducted after staining with Nuclear Fast Red. The known positive sections were selected as the positive control group, whereas PBS, in place of the probe, was used as the negative control group. The lncRNA ANRIL expression levels in kidney tissues of both groups were analyzed using Image J software.

Cell proliferation by CCK-8 assay

Cells (1×10^5 /ml) in a logarithmic phase were inoculated in a 96-well culture plate. After cells in different groups had been treated for 24 h, CCK-8 test was conducted. Absorbance (A) at 450 nm was measured to determine the proliferation index.

Apoptosis detected by flow cytometry

Cells were centrifuged at 1,000 g for 5 min, and the supernatant was discarded. The precipitate was resuspended by addition of 500 μ l of buffer solution. After that, 5 μ l of Annexin V-fluorescein isothiocyanate and 10 μ l of propidium iodide were added to incubate these cells for 5 min at an ambient temperature in the dark. Flow cytometry was performed to detect apoptosis.

Objective protein concentration determination based on western blotting

SDS polyacrylamide gel electrophoresis was used for protein separation. Subsequent to ice-bath transfer of proteins, skim milk powder was sealed for 1–2 h(s) at an ambient temperature. Then, anti-TLR4 (1 : 500), anti-MyD88 (1 : 600), and NF- κ B(p65) (1 : 1000) were added for overnight incubation at 4°C. The next day, the membrane was incubated for 1 h in horseradish peroxidase (HRP)-labeled secondary antibody (anti-rabbit, 1 : 5000) and then washed with TBST before being developed. GAPDH was used as an internal reference in this experiment.

Real-time PCR test

Total RNA was extracted from human blood and kidney tissues of rats in the different study groups, and cells by TRIzol reagent (Invitrogen, USA). To avoid genomic contamination, a PrimeScript 1st Strand cDNA Synthesis Kit containing DNase I (TaKaRa Dalian Branch) was used to carry out RNA reverse transcription and produce the first strand

of cDNA. Real-time PCR amplification was conducted in an ABI 7500 real-time PCR system (Applied Biosystems, USA). Amplimers (lncRNA ANRIL, TLR4, MyD88, NF- κ B [p65]) and GAPDH of internal control were synthesized by GenePharma (Shanghai). An ASYBR Premix Ex Taq kit (TaKaRa, Japan) was used for PCR reactions. The overall reaction volume was 20 μ l and included 2 μ l of cDNA, 10 μ l of 2 \times SYBR Green I PCR master Mix, forward and reverse primer (0.4 μ l each) at a concentration of 10 μ mol/l, 0.4 μ l of ROX Reference Dye and 6.8 μ l of ddH₂O. The thermocycling and amplification conditions include initial denaturation at 95°C for 10 s, followed by 95°C for 5 s, and a final step at 60°C for 34 s, for 40 cycles. The 2^{- $\Delta\Delta$ Ct} method was used to calculate the objective mRNA expression levels. The primer sequences are presented in Table I.

Cell immunofluorescence

4% paraformaldehyde was used to fix cells for 20 min. 3% bovine serum albumin (BSA) was used for mounting for 30 min; and last, NF- κ B(p65) (1 : 100) was added to incubate the cells at 4°C overnight. After washing, fluorescent secondary antibody was added to complete the hybridization. Subsequently, the cells were washed again and mixed with DAPI for 2 min for nuclear staining. Finally, the cells were washed again and mounted using an anti-queching reagent before observation under a fluorescence microscope. DAPI-labeled cell nucleus showed blue fluorescence, while the objective protein showed green fluorescence. For each group of cells, at least 10 fields were randomly chosen to be photographed. Intensity of NF- κ B(p65) staining in the nucleus was analyzed by ImageJ software.

Statistical analysis

Graph plotting was completed based on Graph-Pad Prism 6. 0 (Version X; La Jolla, CA, USA). All data were expressed as mean \pm standard deviation (SD). Data comparison among groups was conducted using ANOVA, and *t*-test was selected for comparison between means. For all analyses, *p* < 0.05 was considered to indicate statistical significance. Statistical analysis was conducted using SPSS software (version 17.0).

Results

ANRIL gene expression levels in groups

lncRNA ANRIL expression levels were significantly higher in the serum of DN patients than in those of the normal group (*p* < 0.001, Figure 1 A). According to RT-qPCR test results of kidney tissues at different time points, lncRNA ANRIL expression levels were also significantly greater in kidney tissues of the DN group than those of

Table I. Relative mRNA primer sequences

Gene name	Primer sequence
ANRIL	F: 5'-CTGATTCAACAGCAGAGATCAAAGA-3'
	R: 5'-CACACCTAACAGTGATGCTTGAAC-3'
TLR4	F: 5'-GGCAGCAGGTGGAATTTGTAT-3'
	R: 5'-CCAAGTTGCCGTTTCTTGT-3'
MyD88	F: 5'-TGAGCAGTCGTGCTGGTATC-3'
	R: 5'-CAGGGCTTTTCTGAGTCGTC-3'
NF- κ B(p65)	F: 5'-GGGAAGGAACGCTGCAGAG-3'
	R: 5'-TAGCCTCAGGGTACTCCATCA-3'
GAPDH	F: 5'-GTCAACGGATTGGTCTGTATT-3'
	R: 5'-AGTCTTCTGGGTGGCAGTGAT-3'

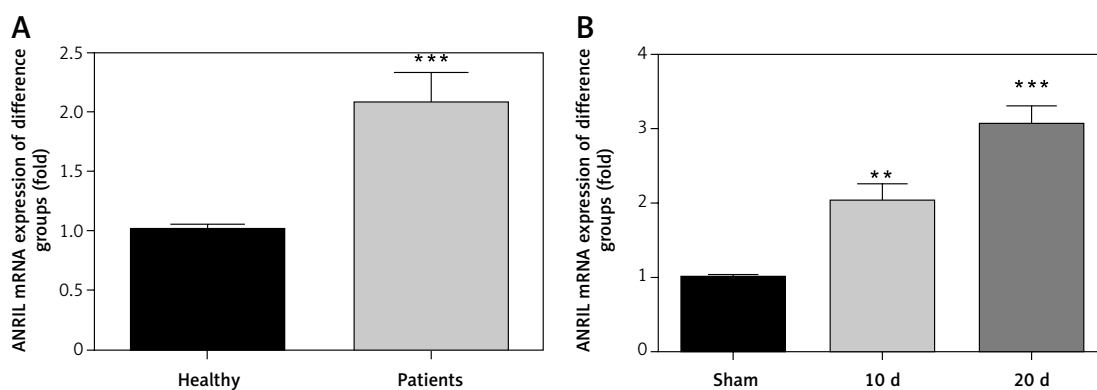


Figure 1. ANRIL gene expression levels in groups. **A** – ANRIL gene expression in difference persons. *** $p < 0.001$ vs. Healthy controls. **B** – ANRIL mRNA expression in kidney tissues of difference rat groups. ** $p < 0.01$ and *** $p < 0.001$ vs. sham group

the sham group on days 10 and 20 ($p < 0.01$ and $p < 0.001$, respectively, Figure 1 B). Moreover, their lncRNA ANRIL expression levels on day 20 were above those on day 10.

Differences in concentrations of LDH, SOD, MDA, IL-6, and TNF- α in rat serum of different groups

The concentrations of LDH, MDA, IL-6, and TNF- α in the rat serum were significantly higher and SOD was significantly lower on day 10 and day 20 after DN model establishment than in the sham group ($p < 0.01$ and $p < 0.001$, respectively; Figures 2 A, B). In addition, LDH, MDA, IL-6, and TNF- α concentrations in rat serum of the DN group on day 20 were much higher and SOD was much lower than those on day 10. These results showed that with increasing duration of DN, the concentrations of LDH, MDA, IL-6, and TNF- α all tended to increase and SOD tended to decrease.

Pathological alterations of kidney tissues

Both the renal cortex and renal medulla are assumed to be structurally normal in the sham group. No abnormalities were found with respect to the sizes and morphology of kidney tubules and glomerulus; further, the tubulointerstitial is free of broadening, obvious hyperemia, or inflammatory cell infiltration. Based on the DM model, the volumes and weights of both kidneys significantly decreased in the rats in the 10-day and 20-day groups, double kidneys with color turning pale harden, and cicatrices are formed. Under a light microscope, extensive glomerular fibrosis could be observed; kidney tubules to which the glomerulus belongs appeared to shrink and even disappear; and proliferation of interstitial fibrous tissues occurred. Due to plasma cell infiltration and fibrous tissue shrinkage, glomeruli with pathological changes drew close to each other, which re-

sulted in concentration. In terms of the remaining comparatively normal glomeruli, compensatory hypertrophy and kidney tubule expansion were observed. Pathological deterioration of rat kidneys in the 20-day group was more severe than that seen in the 10-day group (Figure 3 A).

Apoptosis in rat kidney tissues

The TUNEL assay was used to evaluate apoptosis in kidney tissues of rats in different groups. By comparing results presented in Figure 3 B with those of the sham group, the number of apoptotic cells in the 10-day and 20-day groups showed a significant increase after DN modeling ($p < 0.01$ and $p < 0.001$, respectively; Figure 3 B). Moreover, the maximum quantity of apoptotic cells was found in the kidney tissues of the 20-day group.

ANRIL expression in rat kidneys based on ISH

ANRIL expression levels in the 10-day and 20-day groups were significantly better after DN modeling than the sham group ($p < 0.01$ and $p < 0.001$, respectively; Figure 4 A). In addition, kidney tissues in the 20-day group presented the highest ANRIL expression level.

Differences in TLR4, MyD88, and NF- κ B(p65) protein expression in rat kidneys

IHC was used to test associated proteins in kidney tissues of rats in different groups. When compared with the sham group, protein expression levels of TLR4, MyD88, and NF- κ B(p65) in the rat kidney tissues of the 10-day and 20-day groups were significantly enhanced according to the DN model ($p < 0.01$ and $p < 0.001$, respectively; Figures 4 B–D). The highest protein expression levels of TLR4, MyD88, and NF- κ B(p65) were found in the rat kidney tissues of the 20-day group. The relative data are shown in Figures 4 B–D.

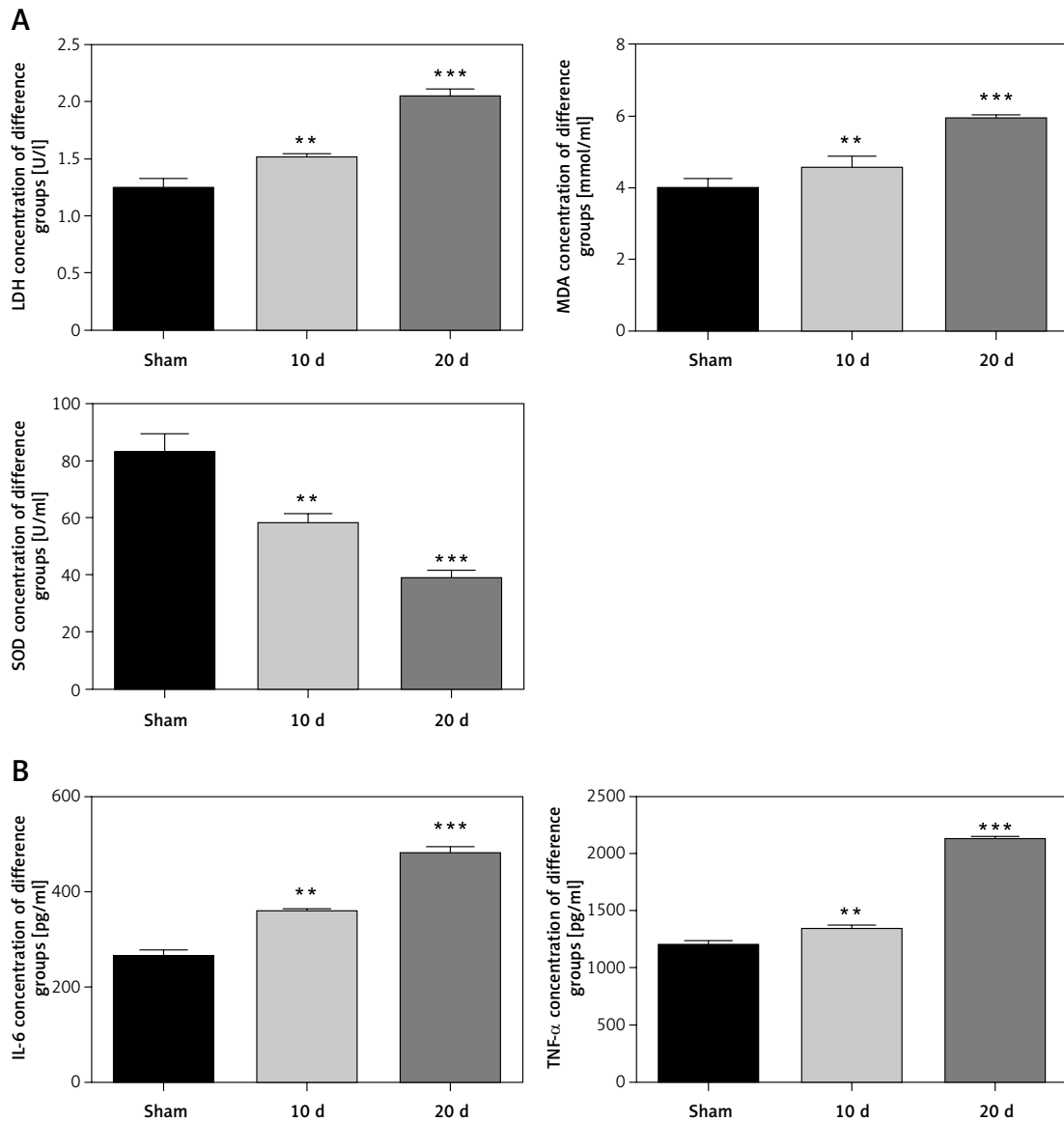


Figure 2. Differences in levels of LDH (A), MDA (B), SOD (C), IL-6 (D), and TNF- α (E) in rat serum from different groups. **A** – LDH, SOD, and MDA concentrations of difference groups. **B** – IL-6 and TNF- α variations of rat serum in different groups

Sham – sham group, 10 d – DN model rats at 10 days, 20 d – DN model rats at 20 days. ** $P < 0.01$ and *** $p < 0.001$ vs. sham group.

Determining mRNA expression levels for related genes in rats

RT-qPCR was used to test related genes in kidney tissues of rats in different groups. The protein expression levels of TLR4, MyD88, and NF- κ B(p65) in rat kidney tissues of the 10- and 20-day groups were significantly higher than those in the sham group ($p < 0.01$ and $p < 0.001$, respectively; Figure 5). The highest protein expression levels of TLR4, MyD88, and NF- κ B(p65) were found among rat kidney tissues of the 20-day group.

LDH, SOD, MDA, IL-6, and TNF- α alterations in cell supernatants of diverse groups

As indicated by ELISA, unlike the NC group, the concentrations of LDH, MDA, IL-6, and TNF- α dramatically increased and SOD significantly decreased in the model and sh-NC groups (all $p < 0.001$; Figures 6 A, B). After shRNA (lncRNA ANRIL inhibitor) was imported into HK-2 cells of a high glucose model through transfection, the concentrations of LDH, MDA, IL-6, and TNF- α were all significantly lower and SOD was significantly higher than those in the model group (all $p < 0.001$; Figures 6 A, B).

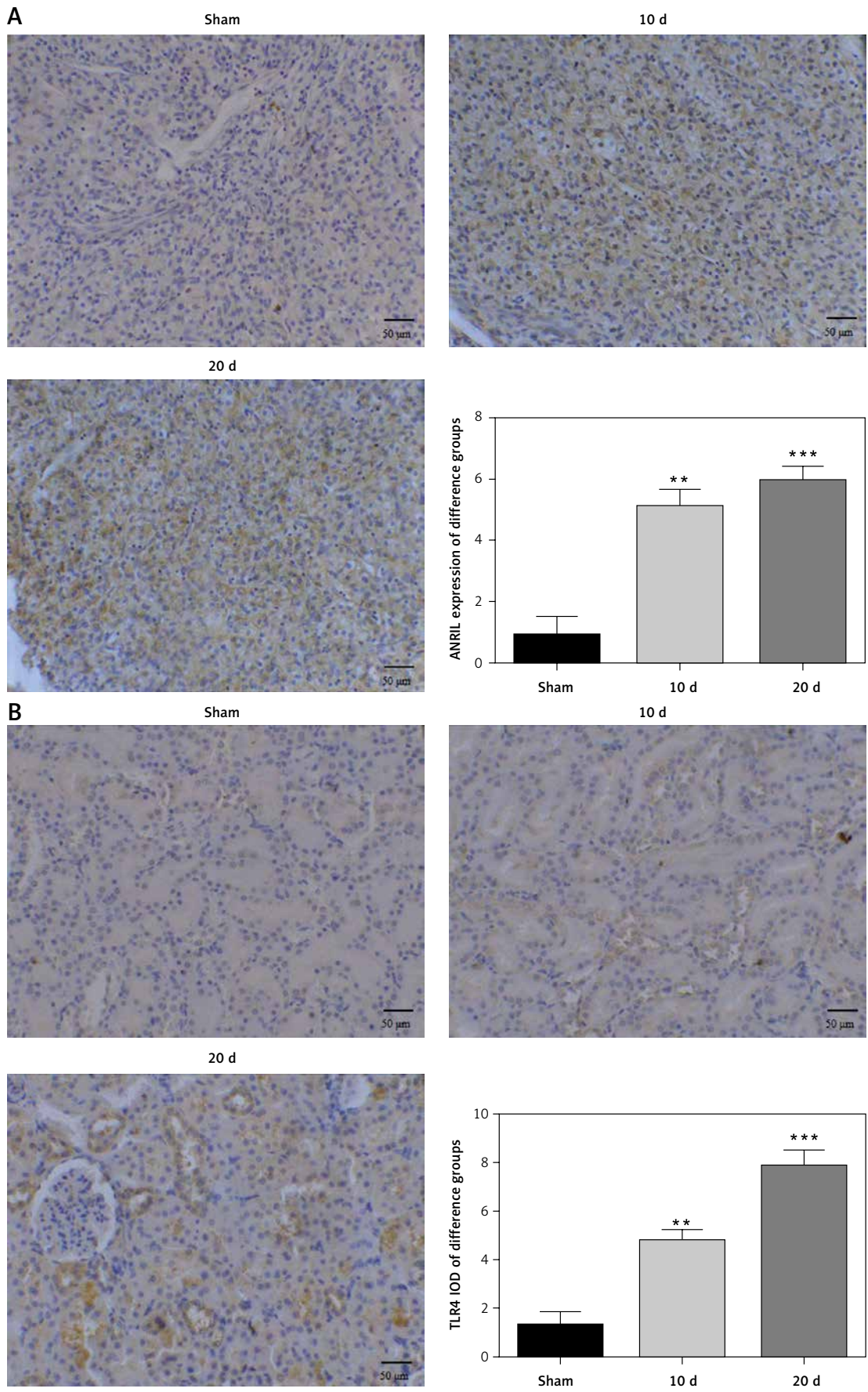


Figure 4. ANRIL and relative protein expression of different groups determined by IHC assay (200×). **A** – ANRIL expression in different groups determined by ISH assay (200×). **B** – TLR4 protein expression in different groups determined by IHC assay (200×)

Sham – sham group, 10 d – DN model rats at 10 days, 20 d – DN model rats at 20 days. ** $P < 0.01$ and *** $p < 0.001$ vs. sham group.

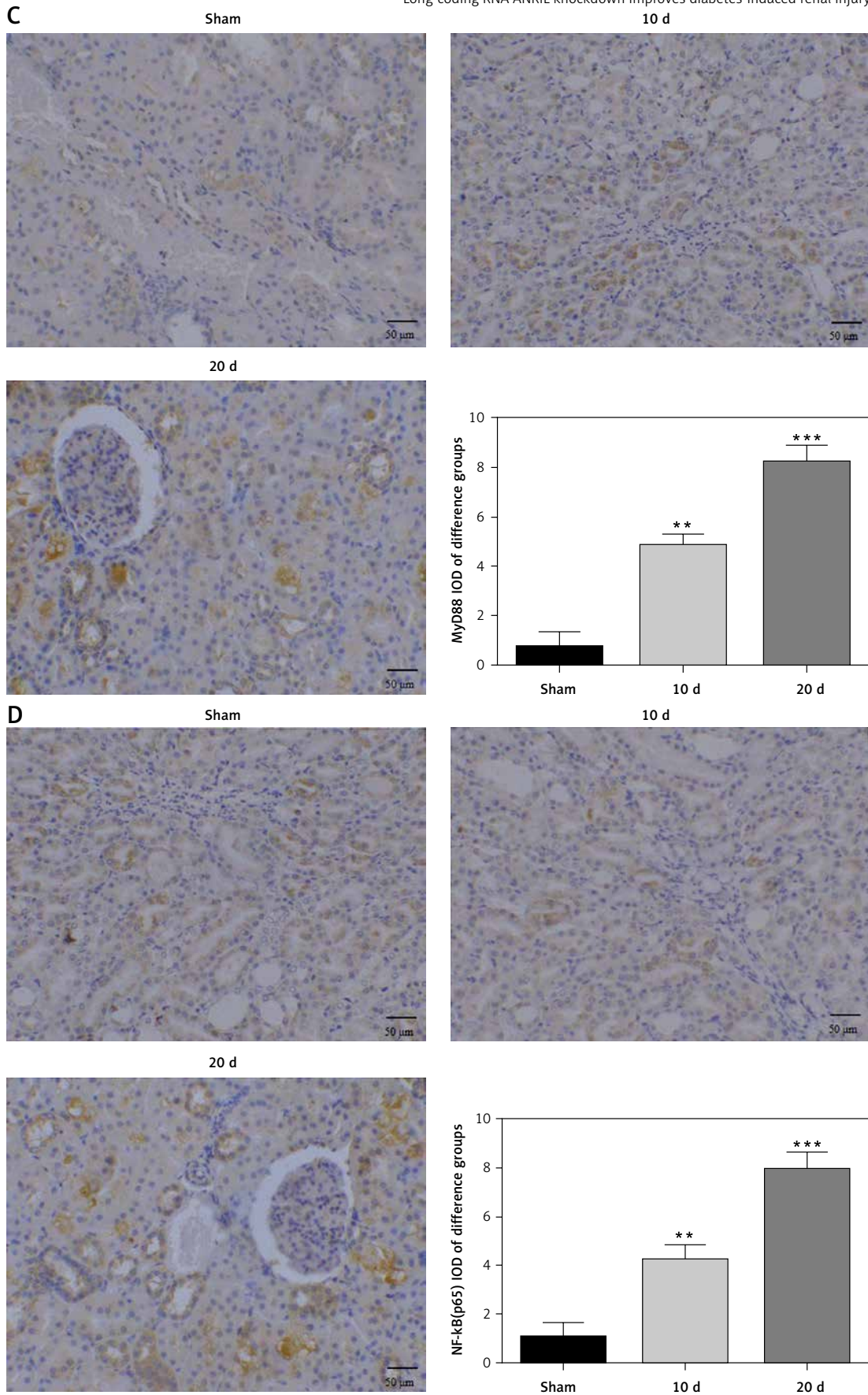


Figure 4. Cont. C – MyD88 protein expression in different groups determined by IHC assay (200×). D – NF-κB(p65) protein expression in different groups determined by IHC assay (200×)

Sham – sham group, 10 d – DN model rats at 10 days, 20 d – DN model rats at 20 days. ** $P < 0.01$ and *** $p < 0.001$ vs. sham group.

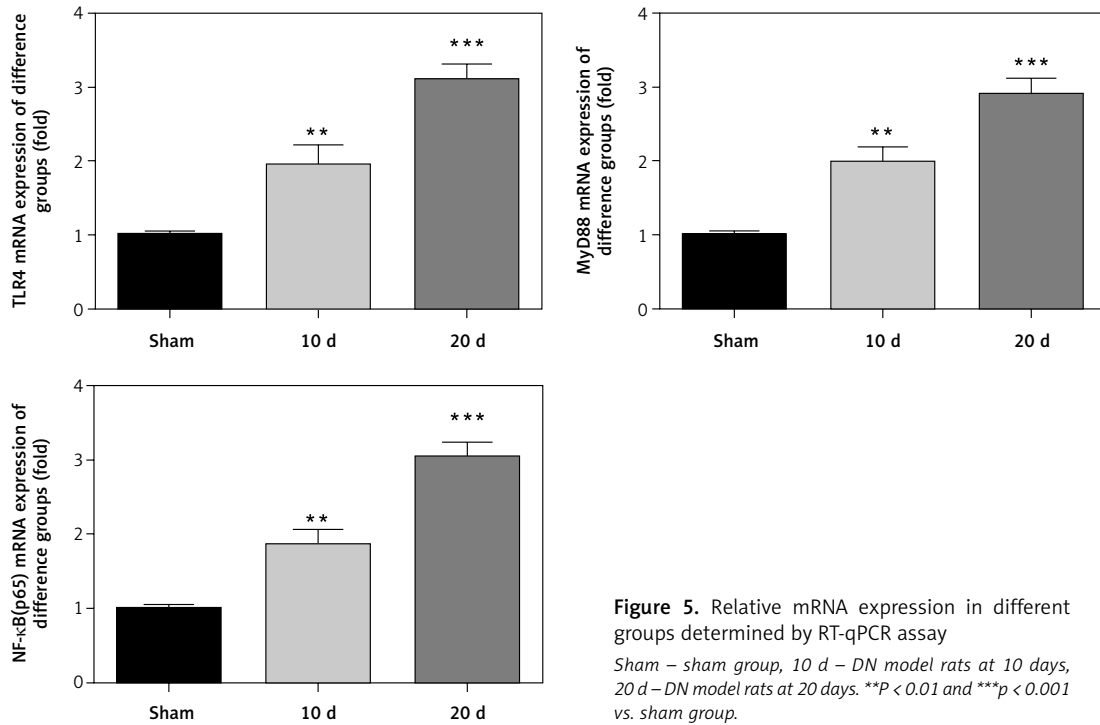


Figure 5. Relative mRNA expression in different groups determined by RT-qPCR assay
 Sham – sham group, 10 d – DN model rats at 10 days, 20 d – DN model rats at 20 days. ** $P < 0.01$ and *** $p < 0.001$ vs. sham group.

Proliferation index and apoptosis rate

The proliferation indices of the model and sh-NC groups were significantly inhibited when compared with the NC group ($p < 0.001$, Figure 7 A). After transfection of shRNA (lncRNA ANRIL inhibitor), the proliferation index of the shRNA group significantly increased, which was not the case for the model group ($p < 0.001$, Figure 7 A). According to the apoptosis rates detected by flow cytometry, significant rises were found in the model and sh-NC groups ($p < 0.001$, Figure 7 B); however, such a phenomenon was absent in the NC group. Subsequent to transfection of shRNA (lncRNA ANRIL inhibitor), the apoptosis rates of the shRNA group were significantly inhibited compared to the model group ($p < 0.001$, Figure 7 B).

Related gene expressions in various cell groups

The expression levels of ANRIL, TLR4, MyD88, and NF-κB(p65)mRNA were significantly improved in the model and sh-NC groups ($p < 0.001$, Figure 8), which is not the case for the NC group. After transfection of shRNA (lncRNA ANRIL inhibitor), the ANRIL, TLR4, MyD88, and NF-κB(p65) mRNA expression levels in the shRNA group were significantly inhibited when compared to the model group ($p < 0.001$, Figure 8).

Associated protein expression levels

In comparison with the NC group, the expression levels of TLR4, MyD88, and NF-κB(p65) mRNA

significantly increased in the model and sh-NC groups ($p < 0.001$, Figure 9). After transfection of shRNA (lncRNA ANRIL inhibitor), their expression levels in the shRNA group were significantly inhibited ($p < 0.001$, Figure 9).

Determining the level of NF-κB(p65) imported into the nucleus

Cellular immunofluorescence was used to determine the amounts of NF-κB(p65) imported into the nucleus. The immunofluorescence in the model and sh-NC groups was significantly higher than in the NC group ($p < 0.001$, Figure 10). After transfection of shRNA (lncRNA ANRIL inhibitor), the amount of NF-κB(p65) imported into the nucleus in the shRNA group was significantly inhibited when compared with the model group ($p < 0.001$, Figure 10).

Discussion

In our research we observed, in the applied animal model, that, as the ANRIL expression level increases, TLR4 and downstream protein expression levels also significantly increase in kidney tissues of rats afflicted by DN. Thus, reduction in ANRIL expression levels may alleviate renal injuries caused by diabetes according to relevant inference. During subsequent experiments, a high glucose model was used to induce HK-2 injuries of the kidney, and shRNA – an lncRNA ANRIL inhibitor – was also imported into cells through transfection. According to corresponding experimental results, proliferation indices in the shRNA group

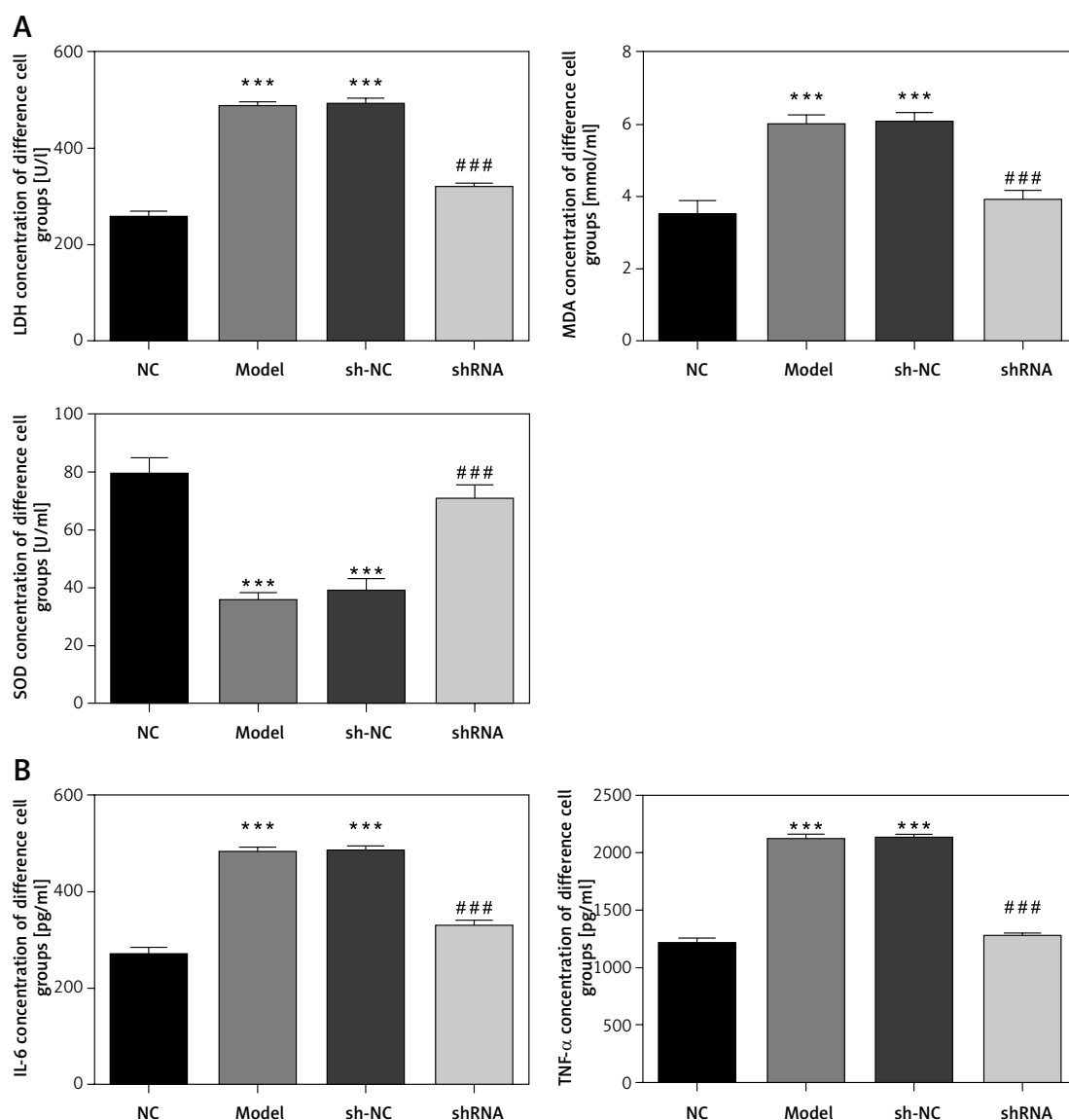


Figure 6. LDH, SOD, MDA, IL-6, and TNF- α alterations in cell supernatants of diverse groups. **A** – LDH, MDA, and SOD concentrations of different groups. **B** – IL-6 and TNF- α concentration of different groups

NC – Normal control group, Model – High glucose-treated group, sh-NC – Cells were transfected with negative control vector based on glucose treatment, shRNA – Cells were transfected with shRNA which knocked down ANRIL based on glucose treatment. *** $P < 0.001$ vs. NC group; ### $p < 0.001$ vs. model group.

were significantly restored, while the apoptosis rate was effectively inhibited. Diabetes is an organ-specific autoimmune disease. Most β cells are damaged by cytotoxic T cells [12]. Early research findings on functions and actions of lncRNA show that it plays a vital role in the organ (e.g., kidneys) development process by regulating key encoding genes associated with development. As research on lncRNA’s mechanism of action in kidney diseases has been conducted in more extensive and profound ways, key actions of lncRNA during the genesis and development of various kidney diseases are being increasingly clarified [13]. In this study, the lncRNA ANRIL mRNA expression levels in serum obtained from DN patients were signifi-

cantly higher than those in the normal population. Also, a rat model of DN was constructed. Renal injuries and inflammation in rats in the model group were more serious with increasing time than those of rats in the sham group. In addition, the ISH and RT-qPCR test results indicated that lncRNA ANRIL expression levels significantly increased in all cases. Accordingly, it can be inferred that lncRNA ANRIL may play an important role during DN development. As a critical sensor, toll-like receptors are critical to both innate and acquired immunity [14]. Therefore, some scholars believe that activation of TLRs not only leads to inflammatory responses but also acts as one of the possible mechanisms that trigger diabetes.

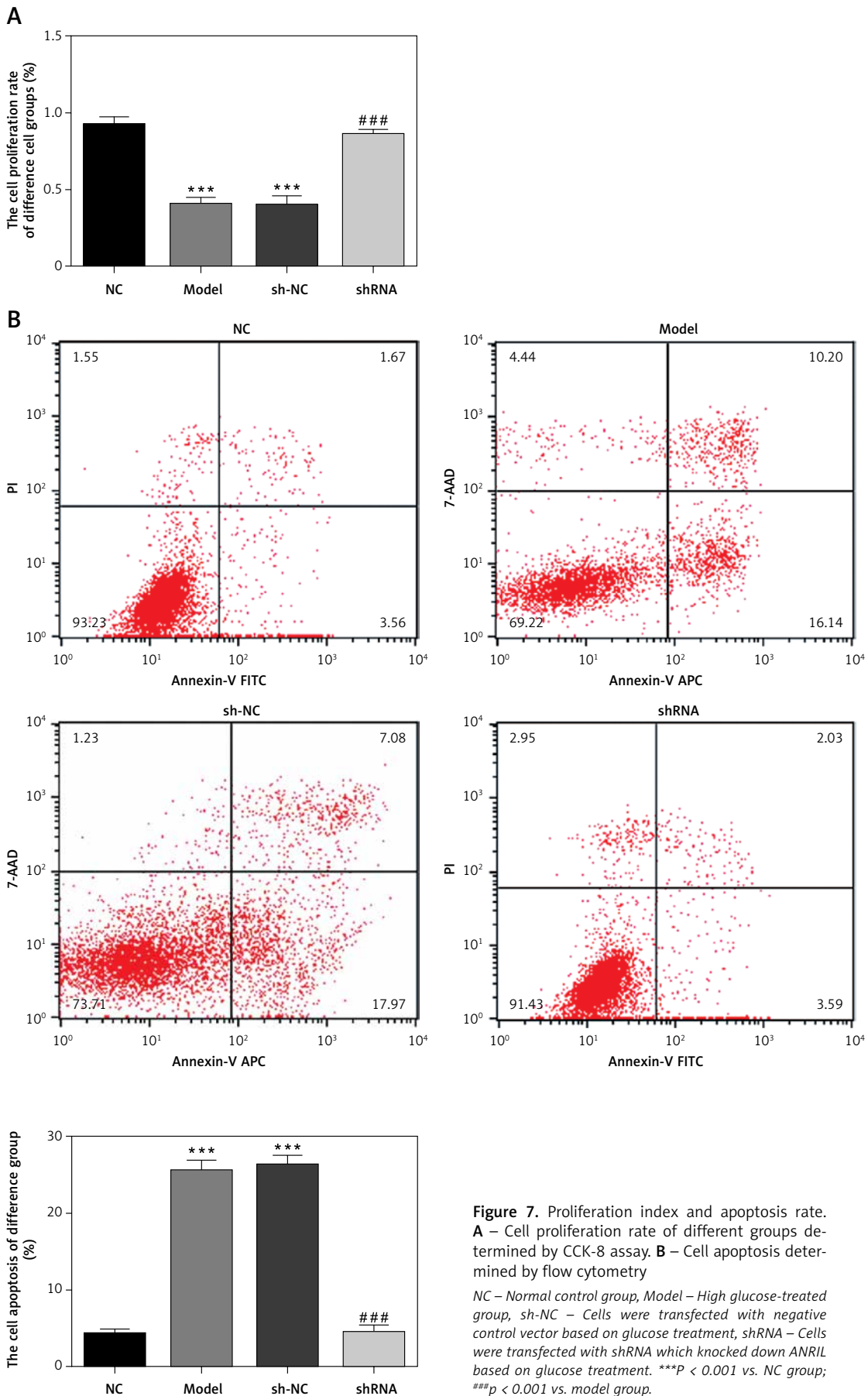


Figure 7. Proliferation index and apoptosis rate. **A** – Cell proliferation rate of different groups determined by CCK-8 assay. **B** – Cell apoptosis determined by flow cytometry. **C** – Cell apoptosis rate of different groups. NC – Normal control group, Model – High glucose-treated group, sh-NC – Cells were transfected with negative control vector based on glucose treatment, shRNA – Cells were transfected with shRNA which knocked down ANRIL based on glucose treatment. *** $P < 0.001$ vs. NC group; ### $p < 0.001$ vs. model group.

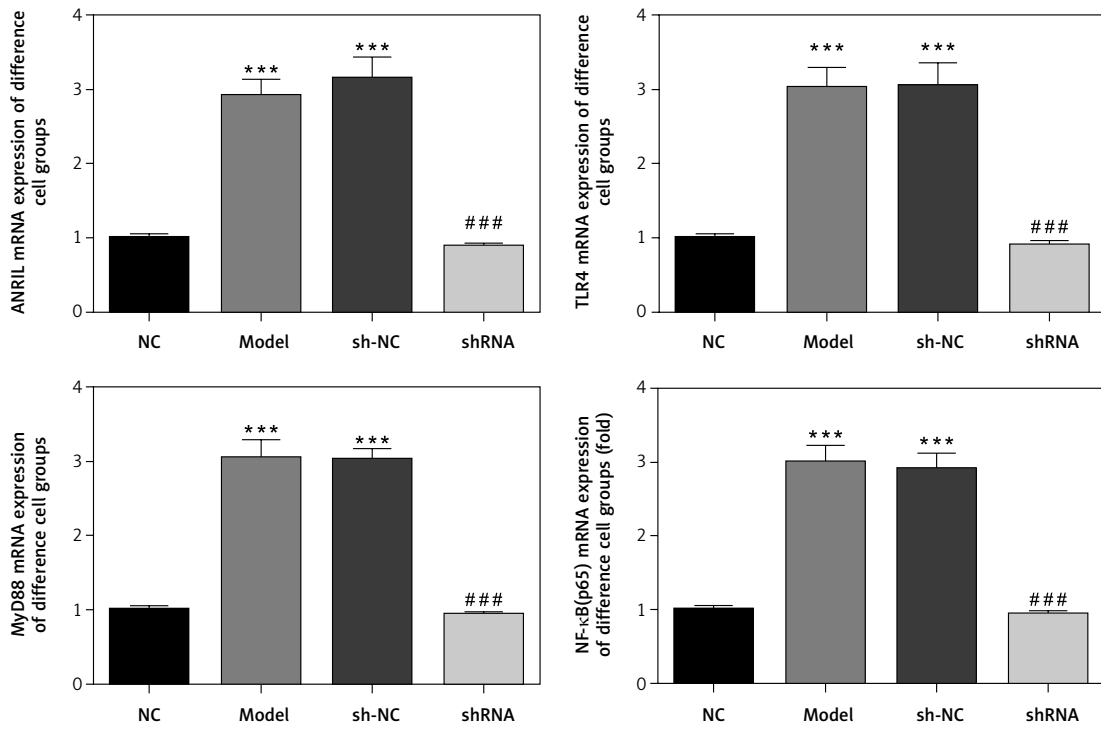


Figure 8. The relative mRNA expression of different groups determined by RT-qPCR assay

NC – Normal control group, Model – High glucose-treated group, sh-NC – Cells were transfected with negative control vector based on glucose treatment, shRNA – Cells were transfected with shRNA which knocked down ANRIL based on glucose treatment. ****P* < 0.001 vs. NC group; ###*p* < 0.001 vs. model group.

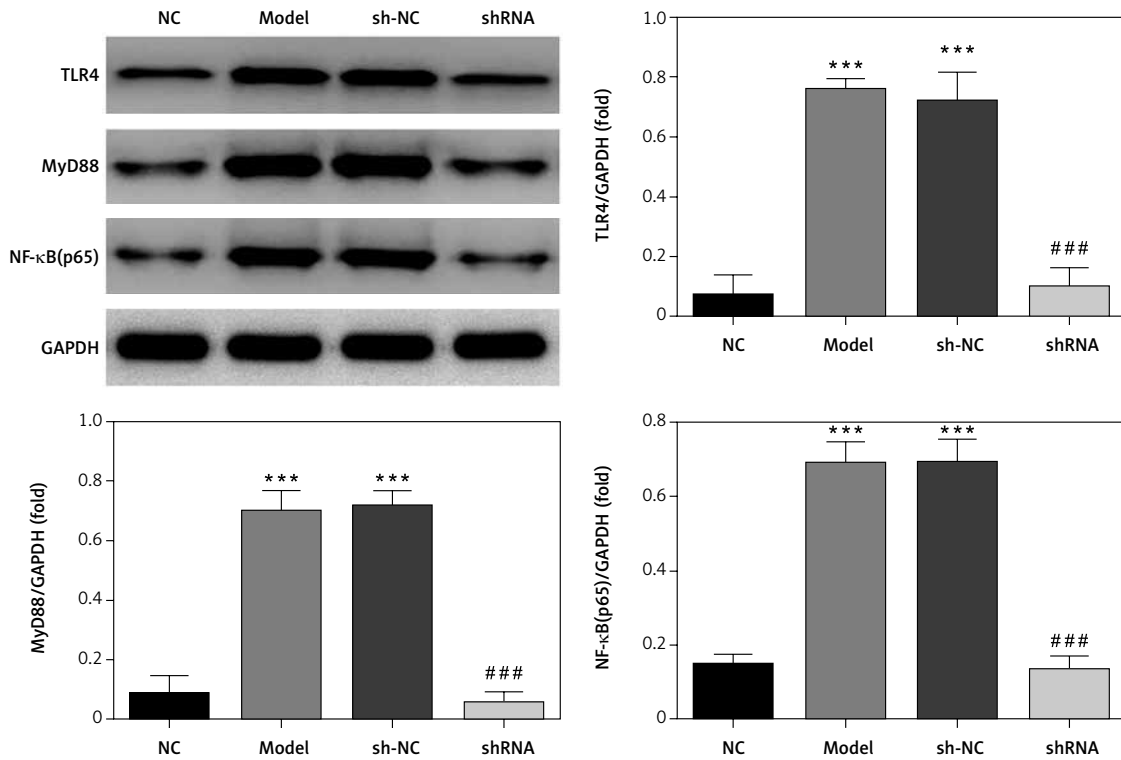


Figure 9. Relative protein expression of different groups by western blotting

NC – Normal control group, Model – High glucose-treated group, sh-NC – Cells were transfected with negative control vector based on glucose treatment, shRNA – Cells were transfected with shRNA which knocked down ANRIL based on glucose treatment. ****P* < 0.001 vs. NC group; ###*p* < 0.001 vs. Model group.

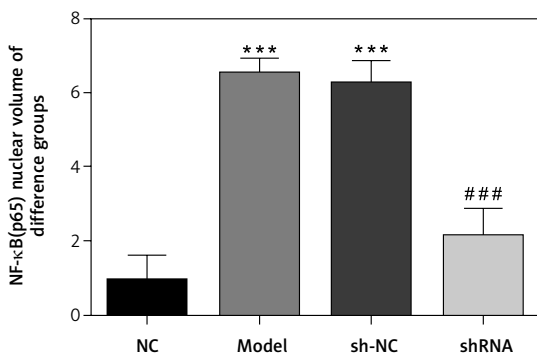
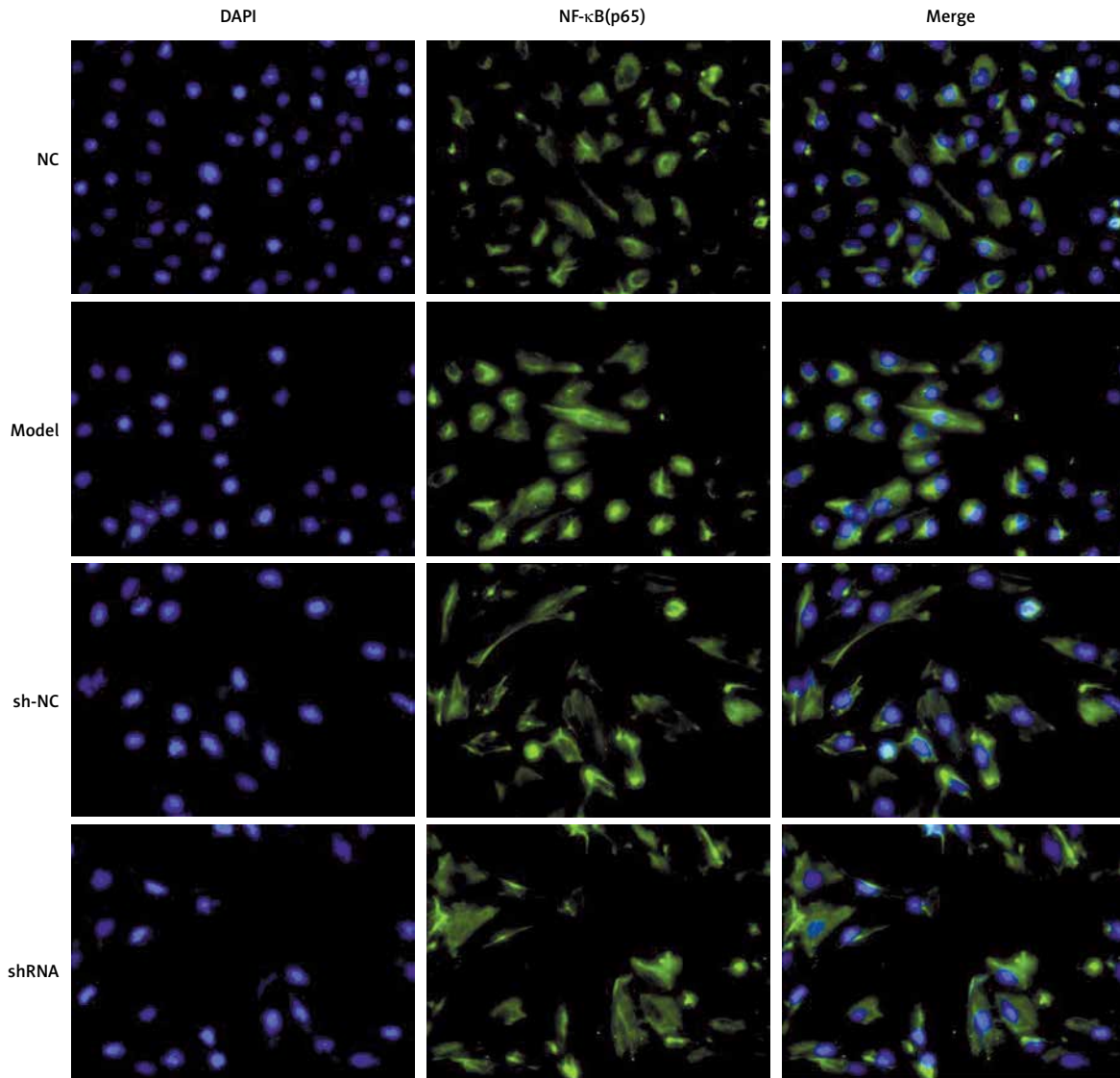


Figure 10. NF-κB(p65) nuclear volume of difference groups

NC – Normal control group, Model – High glucose-treated group, sh-NC – Cells were transfected with negative control vector based on glucose treatment, shRNA – Cells were transfected with shRNA which knocked down ANRIL based on glucose treatment. *** $P < 0.001$ vs. NC group; ### $p < 0.001$ vs. Model group.

Relevant research suggests that TLRs involved in MyD88-dependent signaling pathways activate NF-κB(p65), which gives rise to release of many inflammatory factors. In a diabetic state, the human body experiences high oxidative stress and strong inflammatory responses. Consequently, a significant number of oxygen radicals and inflammatory factors are generated and released, which leads to more severe ischemia-reperfusion injury of viscer-

al organs [15, 16]. As indicated by research findings, activity of both CCK-8 and SOD declines after hypoxia reoxygenation of HK-2 in the presence of high glucose. In this case, the expression levels of LDH, MDA, IL-6, and TNF- α increase, leading to cell viability drop, oxidative stress increase, inflammatory response outburst, and more extensive apoptosis. Subsequent to ANRIL knockdown, the TLR4 expression level is also significantly lowered.

Under such circumstances, not only are partial oxidative stress and inflammatory responses suppressed but also apoptosis is alleviated.

As an important component of the innate immune system, TLRs trigger the onset of diabetes. Statistically, signaling pathways mediated by TLRs are closely related to diabetes and other diseases involving the cardiovascular system, nervous system, liver, and kidneys. In addition, TLRs are involved in the pathogenesis of nephropathy [17, 18]. TLRs have the potential to cooperate with associated signaling molecules and activate cytokine expression, and are also involved in renal injuries caused by immune responses [19].

By activating MyD88-dependent pathways, TLR4 activates NF- κ B(p65) and triggers production of inflammatory cytokines and chemotactic factors. Thus, it finally results in activation of IL-1 receptor associated kinase (IRAK), TNF receptor-associated factor 6 (TRAF6), and TGF- β -activated kinase 1 (TAK1) [20]. As shown by our research findings, in terms of HK-2, protein expression levels of TLR4, MyD88, and NF- κ B(p65) are enhanced as lncRNA ANRIL expression levels increase in an environment of high glucose; consequently, cellular damage becomes more serious. In the same condition, shRNA is imported into cells through transfection. Subsequently, the expression levels of both MyD88 and NF- κ B(p65) decline; the amount of NF- κ B(p65) imported into the nucleus is also significantly inhibited; cell viability is improved; and apoptosis is alleviated. Therefore, TLR4 up-regulation in HK-2, which is caused by high glucose, activates the TLR4/MyD88/NF- κ B(p65) signaling pathway and further exacerbates HK-2 damage. However, ANRIL inhibition has the potential to effectively block the TLR4/MyD88/NF- κ B(p65) signaling pathway, downregulate the expression levels of MyD88 and NF- κ B(p65), and alleviate cellular damage.

In conclusion, lncRNA ANRIL plays a vital role in HK-2 cell injury mechanisms induced by high glucose.

Acknowledgments

Xiaoming Jiang and Nan Su contributed equally to this study.

Conflict of interest

The authors declare no conflict of interest.

References

1. Ho J, Chan H, Wong SH, et al. The involvement of regulatory non-coding RNAs in sepsis: a systematic review. *Crit Care* 2016; 20: 383.
2. Long J, Badal SS, Ye Z, et al. Long noncoding RNA Tug1 regulates mitochondrial bioenergetics in diabetic nephropathy. *J Clin Invest* 2016; 126: 4205-18.
3. Yang Y, Cai Y, Wu G, et al. Plasma long non-coding RNA CoroMarker, a novel biomarker for diagnosis of coronary artery disease. *Clin Sci* 2015; 129: 675-85.
4. Kumarswamy R, Bauters C, Volkman I, et al. Circulating long noncoding RNA, LIPCAR, predicts survival in patients with heart failure. *Circ Res* 2014; 114: 1569-75.
5. Tang W, Zhang D, Ma X. RNA-sequencing reveals genome-wide long non-coding RNAs profiling associated with early development of diabetic nephropathy. *Oncotarget* 2017; 8: 105832-47.
6. Zhou X, Yin C, Dang Y, et al. Identification of the long non-coding RNA H19 in plasma as a novel biomarker for diagnosis of gastric cancer. *Sci Rep* 2015; 5: 11516.
7. de Kok JB, Verhaegh GW, Roelofs RW, et al. DD3(PCA3), a very sensitive and specific marker to detect prostate tumors. *Cancer Res* 2002; 62: 2695-8.
8. Li X, Zhao Z, Gao C, et al. The diagnostic value of whole blood lncRNA ENST000005503373 for pre-diabetes and type 2 diabetes mellitus. *Exp Clin Endocrinol Diabetes* 2017; 125: 377-83.
9. Hu J, Wang D, Wu H, et al. Long non-coding RNA ANRIL-mediated inflammation response is involved in protective effect of rhein in uric acid nephropathy rats. *Cell Biosci* 2019; 9: 11.
10. Guo F, Tang C, Li Y, et al. The interplay of lncRNA ANRIL and miR-181b on the inflammation-relevant coronary artery disease through mediating NF- κ B signalling pathway. *J Cell Mol Med* 2018; 22: 5062-75.
11. Aarabi G, Zeller T, Heydecke G, et al. Roles of the Chr.9p21.3 ANRIL locus in regulating inflammation and implications for anti-inflammatory drug target identification. *Front Cardiovasc Med* 2018; 5: 47.
12. Needell JC, Zipris D. Targeting innate immunity for type 1 diabetes prevention. *Curr Diab Rep* 2017; 17: 113.
13. Lorenzen JM, Thum T. Long noncoding RNAs in kidney and cardiovascular diseases. *Nat Rev Nephrol* 2016; 12: 360-73.
14. Chen JQ, Szodoray P, Zehner M. Toll-like receptor pathways in autoimmune diseases. *Clin Rev Allergy Immunol* 2016; 50: 1-17.
15. Shen X, Hu B, Xu G, et al. Activation of Nrf2/HO-1 pathway by glycogen synthase kinase-3 β inhibition attenuates renal ischemia/reperfusion injury in diabetic rats. *Kidney Blood Press Res* 2017; 42: 369-78.
16. Neelofar K, Arif Z, Arafat MY, et al. A study on correlation between oxidative stress parameters and inflammatory markers in type 2 diabetic patients with kidney dysfunction in north Indian population. *J Cell Biochem* 2019; 120: 4892-902.
17. Kasimsetty SG, McKay DB. Ischemia as a factor affecting innate immune responses in kidney transplantation. *Curr Opin Nephrol Hypertens* 2016; 25: 3-11.
18. Alibashe-Ahmed M, Roger T, Serre-Beinier V, et al. Macrophage migration inhibitory factor regulates TLR4 expression and modulates TCR/CD3-mediated activation in CD4⁺ T lymphocytes. *Sci Rep* 2019; 9: 9380.
19. Wei X, Liu H, Li X, et al. Over-expression of miR-122 promotes apoptosis of hepatocellular carcinoma via targeting TLR4. *Ann Hepatol* 2019; 18: 869-78.
20. Cano A, Mattana A, Woods S, et al. Acanthamoeba activates macrophages predominantly through Toll-like receptor 4- and MyD88-dependent mechanisms to induce interleukin-12 (IL-12) and IL-6. *Infect Immun* 2017; 85: e01054-16.